Heart Surgery Forum 2024; 27(5): E473–E482
doi: 10.59958/hsf.7399
https://journal.hsforum.com/

Article

Mechanical Analysis of the Connection Structure of a Double-Layered Valve Stent within an Annuloplasty Ring

Ke Dong[1], Zhaoming He[2,*]

[1]Department of Biomedical Engineering, Research Center of Fluid Machinery Engineering and Technology, Jiangsu University, 212013 Zhenjiang, Jiangsu, China
[2]Department of Mechanical Engineering, Texas Tech University, Lubbock, TX 79409, USA
*Correspondence: 1000004151@ujs.edu.cn (Zhaoming He)

Submitted: 1 March 2024 Revised: 26 March 2024 Accepted: 8 April 2024 Published: 12 May 2024

Abstract

Background: In this study, to address the failure of mitral valve repair surgery, a novel valve-in-ring model for an artificial mitral valve annuloplasty ring and a new double-layer mitral valve were established. A suitable number and length of ventricular fixation struts within the annuloplasty ring, as well as the implantation depth, result in variations in stress and strain for the inner and outer stent layers. **Methods**: The compression and self-expansion model of the stent was established via finite element analysis. The changes in stress and strain were analyzed by setting the length and number of the ventricular fixed struts and implantation depth. **Results**: When only affected by factors such as blood pressure, the maximum stresses of stent structures with three and six ventricular fixed struts are 476 and 222 MPa, respectively, in the right posterior annular region. At implantation depths of 0, 0.5, 1, and 2 mm, the maximum stresses are located in the left posterior annular region of the outer stent and are 740, 697, 709, and 742 MPa, respectively, and the maximum displacements of the inner stent are all in the right posterior ventricular fixed strut region of the posterior annulus and are 3.71, 3.10, 2.48, and 1.87 mm, respectively. In the three and six ventricular fixed strut stents, when the ventricular fixed strut length is 3, 4, and 5 mm, the maximum stresses are 570, 557, and 621 MPa and 674, 666, 644 MPa, respectively. **Conclusions**: Appropriately increasing the number of ventricular fixed struts can effectively reduce damage to the stent inside the body, and the damage to the stent is relatively consistent across different implantation depths; however, the right side of the stent's posterior annulus is particularly susceptible to damage. However, if the implantation depth is lower, the impact on the inner stent will be more significant. As the number of ventricular fixed struts increases, the strut length variation has a relatively stable impact on stent damage.

Keywords

valve-in-ring model; double-layer mitral valve; mitral valve; finite element analysis; mitral annuloplasty ring

Introduction

Mitral valve repair surgery, a type of transcatheter mitral valve repair, is a common method for treating mitral functional regurgitation [1]. Functional mitral regurgitation is typically caused by structural changes resulting from factors such as anterior leaflet displacement and left ventricular dilation, leading to incomplete mitral valve anterior and posterior leaflet closure. Mitral valve annuloplasty, a type of mitral valve repair surgery, aims to restore the dilated native mitral valve to its original size, thereby allowing proper anterior and posterior leaflet closure. This procedure is performed to improve regurgitation. However, artificial mitral valve ring failure often occurs owing to instrument aging, cracking, and other factors [2]. In addition, considering that patients with this condition are generally older, surgical thoracotomy is inappropriate for reflux. Transcatheter mitral valve replacement (TMVR) has become one of the most effective alternative treatment for mitral regurgitation [3]. The treatment method for reimplanting a valve stent in an annuloplasty ring is clinically referred to as "Valve-In-Ring" (VIR), and a significant amount of clinical data have shown that the VIR treatment approach is feasible [4,5]. Currently, it is unclear how the stent design and implantation depth under these physical conditions affect the hemodynamic and mechanical properties of VIR stents. Moreover, precise conclusions are lacking in clinical practice.

Good performance of mitral valve stent products needs to meet many conditions [6] and be capable of being pressed into a delivery system; the stress on the stent must be lower than the ultimate tensile strength of the stent material after implantation; it must maintain good hemodynamic performance; and the radial support force of the stent must not damage the mitral ring. Currently prevalent aortic intervention valves used in clinical practice have a circular cross-sectional shape [7]. Circular stents cannot expand into their original shape after implantation, which leads to problems such as poor valve lobe closure and lack of tight fitting with the forming ring. While D-shaped and elliptical stents may be similar to the mitral valve structure, their hemodynamic performance is inferior to that of circular stents [8,9]. Therefore, conventional aortic intervention valves are not suitable for mitral valve implantation.

In this paper, a new double-layer mitral valve stent is proposed. The connection structure in which the inner valve stent connects with the outer anchor stent through rivets is referred to as a ventricular fixation strut. The inner stent was designed to be round for good hemodynamic performance, and the outer stent was designed to be D-type to match the primary mitral valve structure [5,6]. Differences in the morphological ventricular fixed strut design affect the stent performance, and changes in the number of ventricular fixed struts affect its efficiency. If the number of fixed ventricular struts is too small, adverse phenomena might occur, such as falling off of the inner valve stent, excessive concentration force, and stent damage [10]. If the number of struts is too large, the stent will be excessively distorted and damaged when forced into the delivery system, which affects its life and hemodynamic performance, especially for stents with different inner and outer cross-sections. In addition, slight changes in the ventricular fixation strut length can affect the lifetime and other characteristics of stents, which are expected to function for ten years. However, there is a lack of research on the number and length of fixed ventricular struts with different cross-sectional shapes.

Therefore, the main purpose of this study was to evaluate various aspects of mitral valve stent treatment within the annuloplasty ring by analyzing the impact of different numbers and lengths of ventricular fixation struts as well as varying implantation depths into the ring for a novel double-layer mitral valve stent. The detailed goals of this study can be summarized as follows: (1) Investigate the influence of varying numbers of ventricular fixation struts on the stress and strain experienced by a double-layer stent throughout one cardiac cycle. (2) Analyze the stress and strain distribution of the stent after implantation into a shaping ring with different numbers and lengths of ventricular fixation struts, providing data for subsequent stent research. (3) Examine the stress and strain distribution of the valve stent within the ring at different implantation depths and determine the optimal implantation depth, offering data-driven guidance for clinical interventions involving valve surgery within the ring.

Materials and Methods

Three-Dimensional Modeling

The annuloplasty ring model is referenced from the 36-mm Physio Annuloplasty Ring, which has been extensively used clinically by the Edward Company, and is reconstructed three-dimensionally using SolidWorks, as shown in Fig. 1.

A new type of VIR stent was designed for the annuloplasty ring, as shown in Fig. 2; it consists of an inner valve stent, ventricular fixation struts, and an outer anchoring stent, in which the outer anchoring stent also contains anchoring hooks. The inner valve stent is designed as

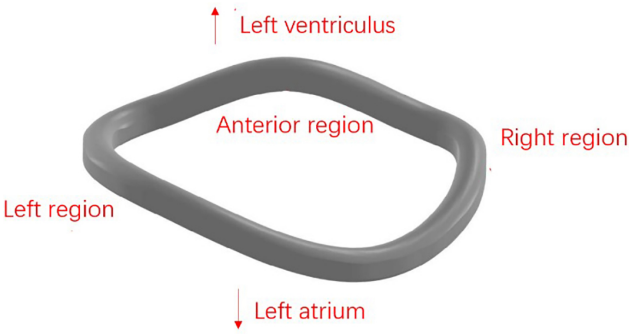

Fig. 1. Annuloplasty ring model.

a round shape to ensure good hemodynamic performance, similar to the interventional aortic valve. To fix the in-ring stent in the annuloplasty ring and avoid falling off, the outer anchoring stent is designed to be D-shaped, similar to the three-dimensional ring structure, and its perimeter is approximately 12 mm longer than the inner perimeter of the annuloplasty ring. Furthermore, an anchor hook was placed at the bottom. The function of the ventricular fixation struts is to connect the inner and outer stents, and their mode of action is rivet binding. Considering the connection stability and damage reduction caused by excessive restraint to the stent, the number of ventricular fixed struts was designed to be three and six, respectively. All models were drawn in SolidWorks, and the specific dimensions are shown in Fig. 3 and listed in Table 1 (Ref. [11]).

Table 1. Stent parameters [11].

Parameter	Value
Inner stent diameter D_0/mm	24.20
Stent wall thickness T_0/mm	0.40
Outer stent transverse diameter D_1/mm	37.00
Outer stent vertical diameter H_1/mm	27.00
Outer stent wall thickness T_1/mm	0.40
Anchor hook diameter for the outer bracket r_1/mm	3.00
Ventricular fixation strut length H/mm	3.00, 4.00, 5.00

Materials and Mesh Modeling

Because the annuloplasty ring deformation was not considered in this study, the mesh properties of the annuloplasty ring were set to be rigid. Currently, these materials are commonly used in clinical applications, including medical stainless steel, tantalum metal, nitinol alloys, and degradable polymers. However, because we used a double-layer stent, which is suitable for self-expanding mode, a nitinol alloy was used in the design.

In industrial applications, the shape and temperature can be linked by changing the carbon content of nickel-titanium alloys. When the temperature reaches a critical state, the Ni–Ti alloy can restore its original shape. The nitinol alloy density is 6.5×10^{-9} mm^3; its Young's mod-

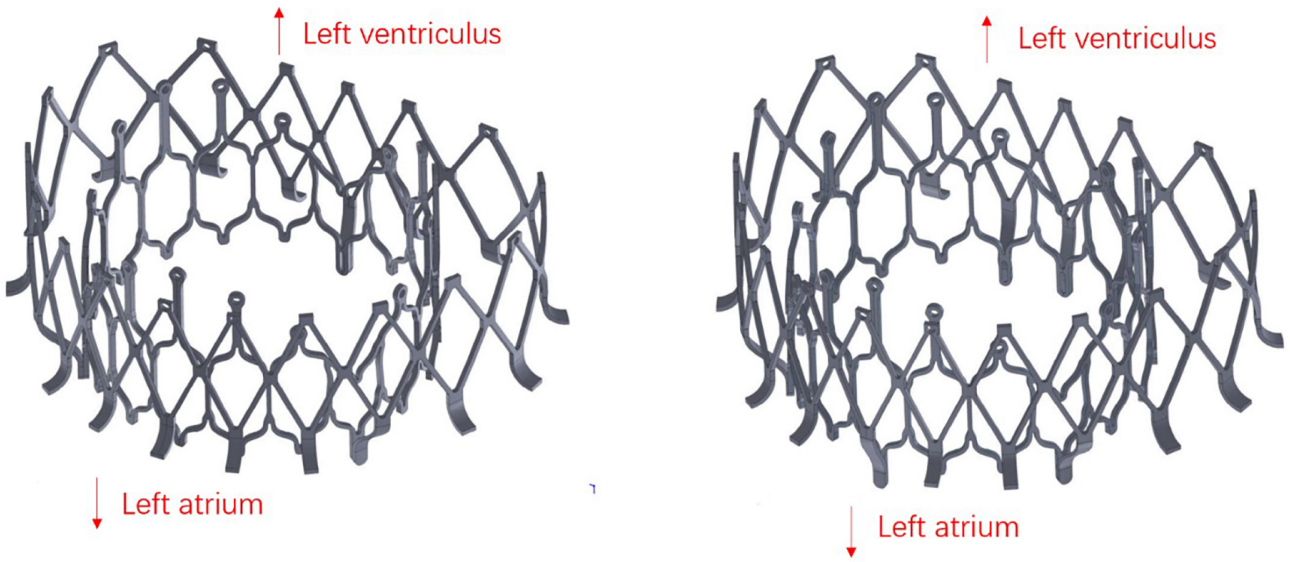

Fig. 2. Double-layer stent models with three and six ventricular fixed struts.

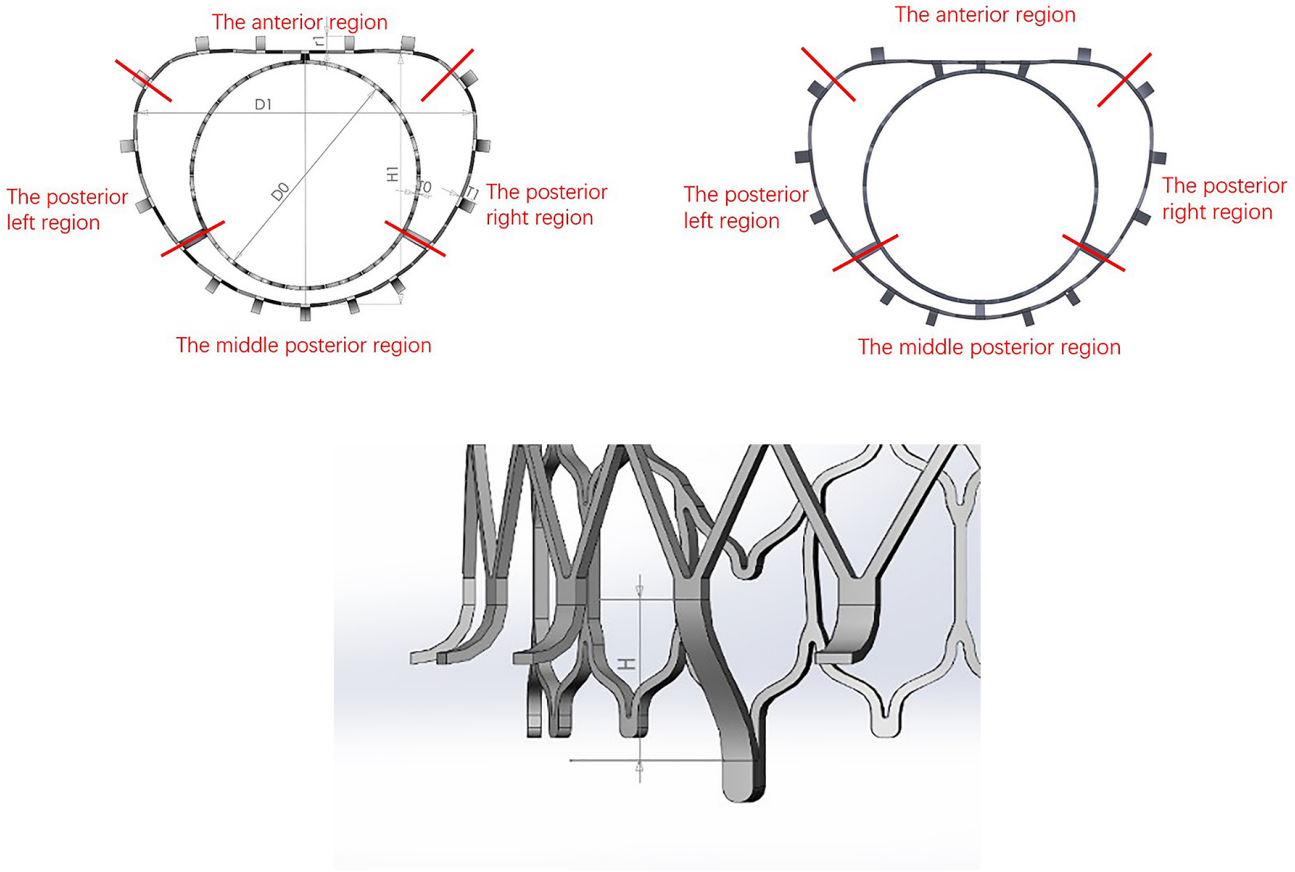

Fig. 3. Schematic of the stent dimensions.

ulus and Poisson's ratio are 51,700 and 0.3, respectively. In Abaqus, the constitutive equation of the Superelasticity model was used to endow the scaffold with superelastic properties; the specific parameters are listed in Table 2.

The grid adopts an 8-node hexahedral linear reduction integral element (C3D8R), which is resistant to the shear self-locking phenomenon, yields a more accurate displacement solution, and can effectively ensure the calculation convergence and accuracy of the results. To avoid mesh factors affecting the results, the stent mesh size was set to 0.08.

Table 2. Nitinol parameters.

Parameter	Value
Martensite Young's modulus/MPa	47,800
Martensite Poisson's ratio	0.3
Transformation strain	0.063
Transformation loading start/MPa	600
Transformation loading end/MPa	670
Transformation unloading start/MPa	288
Transformation unloading end/MPa	254
Transformation loading start in compression/MPa	900
Reference Temperature/°C	37
Loading	6.527
Unloading	6.527
Volumetric transformation	0.063

Finite Element Analysis (FEA) Modeling

Because the stress and strain caused by the transvalvular pressure gradient and other factors on the stent change according to the number of ventricular fixed struts, the Abaqus display static analysis method was used in the simulation to calculate the stent stress magnitude and concentration area after stress and to find the most vulnerable area in the cardiac cycle. In the boundary condition module, a new cylindrical coordinate system was created (the axial direction of the inner support is Z, the radial direction is R, and the circumferential direction is T), and the axial rotation of the top section of the outer support was set to zero. A 15-N axial upward force was applied to the bottom surface of the inner stent (the pressure exerted on the stent by factors such as blood pressure during a cardiac cycle was less than 15 N), as shown in Fig. 4.

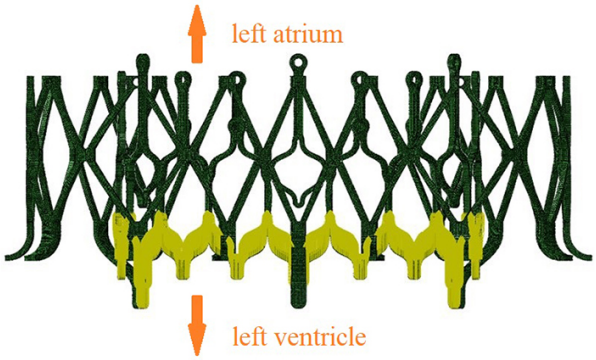

Fig. 4. Stent compressed solely by factors such as blood pressure.

To save computational time and enhance computational convergence, Abaqus was used to display the simulation dynamic analysis to calculate the stent performance, obtain the stent mechanical trends for different numbers and lengths of ventricular struts when implanted in the annuloplasty ring, and obtain the best implantation depth for the mid-annular valve stent. The entire calculation is divided into two steps: (1) The double-layer mitral valve stent is placed in the clamping shell model, and the clamping shell radial clamping is commanded to 35 Fr to simulate the process of the stent being pressed into the delivery system, as shown in Fig. 5. (2) To reduce the model calculations, the slow release process of the stent from the delivery system is simplified to the direct removal of the clamping shell, as shown in Fig. 6a. The temperature field variable is set to 37 °C to simulate the process of self-expansion of the double-layer mitral valve stent and contact with the ring *in vivo*. The best implantation depth was determined by imitation of the flap. The implantation depth, which is the distance between the bottom of the annuloplasty ring and the bottom of the outer surface of the anchoring hook, as represented by the distance between the two red lines (in Fig. 6b) was set to 0, 0.5, 1, and 2 mm.

Results

Stress Analysis for Three- and Six-Ventricular Fixed-Strut Stent

With three and six ventricular fixed struts, the stress of the stent caused only by blood pressure and other factors was 476 and 318 MPa, respectively, which is less than the ultimate tensile strength of the nickel-titanium memory alloy (1290 MPa), as shown in Fig. 7. The high stress of the three- and six-ventricular fixed-strut stents was mainly concentrated in the ventricular fixed struts of the outer stent. Specifically, the maximum stress on the middle side of the anterior region of the three-ventricular fixed struts was 349 MPa, and the maximum stress on the left and right sides of the posterior region was 476 MPa. The maximum stress of the anterior region of the six-fixed ventricular struts was 137 MPa, and the maximum stresses on the middle side and both sides of the posterior region were 182 and 222 MPa.

In the three- and six-ventricular fixed-strut stents, the high-strain area of the inner stent is in the part connected with the ventricular connecting struts. The maximum strains of the anterior region and both sides of the posterior region of the three-ventricular fixed-strut inner stents were 0.28% and 0.47%, respectively. The maximum strains of the inner stent in the anterior region, both sides of the posterior region, and the middle of the posterior region were 0.31%, 0.22%, and 0.20%, respectively.

Stress and Strain Analysis of the Three-Ventricular Fixed-Strut Stent Implanted at Different Annuloplasty Ring Depths

The stress distribution of the three-ventricular fixed-strut stent with a length of 4 mm at different implantation depths is shown in Fig. 8. The maximum stresses were 742, 697, 709, and 742 MPa at implantation depths of 0, 0.5, 1, and 2 mm, respectively, and all were located in the left region of the posterior ring of the outer stent.

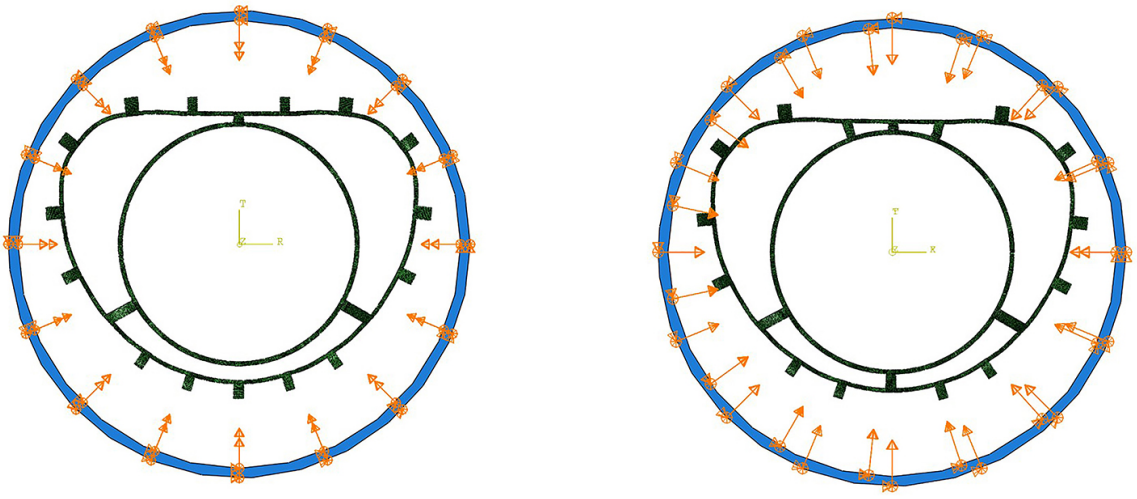

Fig. 5. Diagram of the stent press grip model. R, the radial direction; T, the circumferential direction.

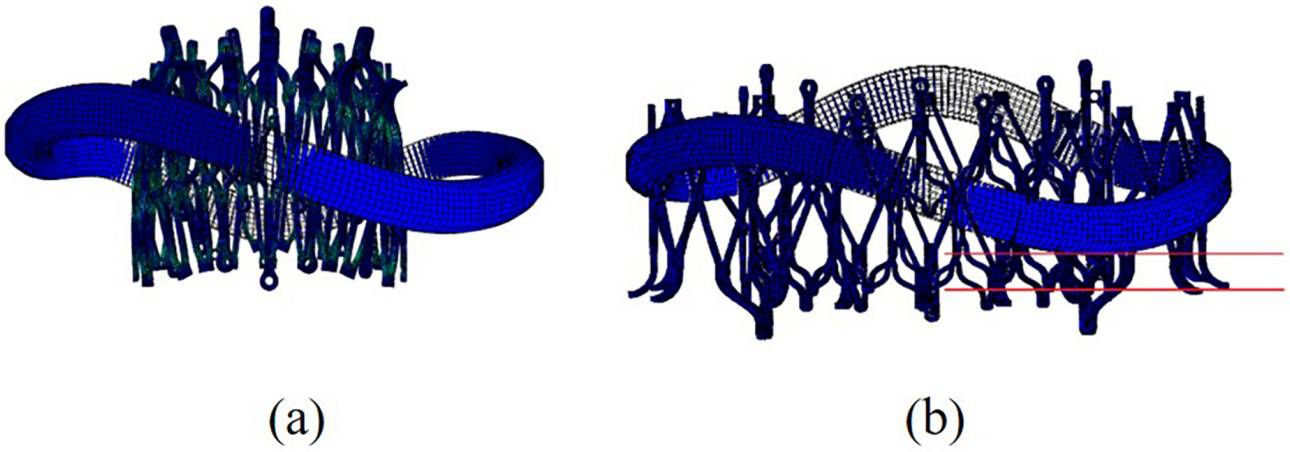

Fig. 6. Diagram of stent implantation procedure. (a) Self-expanding mitral valve stent model. The distance between the two red lines in (b) represents the implantation depth.

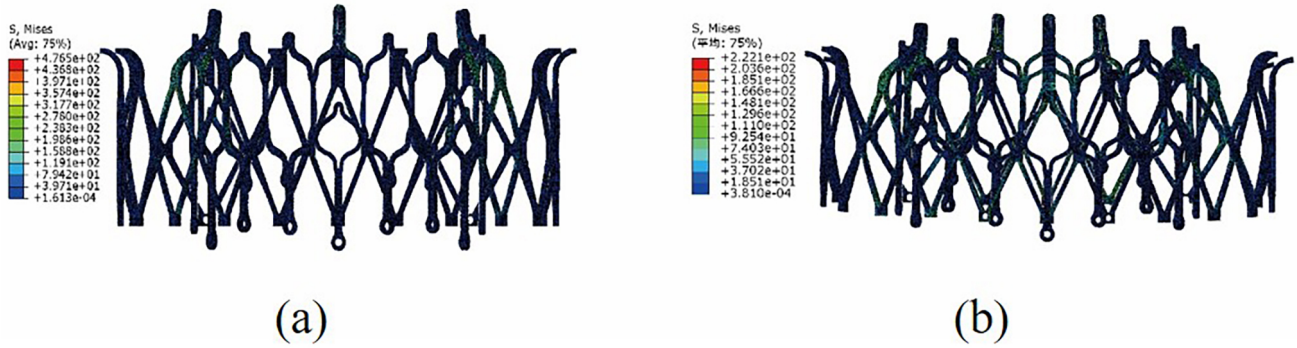

Fig. 7. Stress analysis diagrams for (a) three- and (b) six-ventricular fixed struts, respectively, which are only affected by factors such as blood pressure.

The displacement of the three-ventricular fixed-strut inner stent implanted at different annuloplasty ring depths is shown in Fig. 9. The maximum stent displacements implanted at 0, 0.5, 1, and 2 mm were 3.71, 3.10, 2.48, and 1.87 mm, respectively, and all were in the right ventricle fixed strut of the posterior region. The maximum displacements of the left ventricular fixed strut in the posterior region of the stent were 0.43, 0.80, 0.84, and 0.77 mm, re-

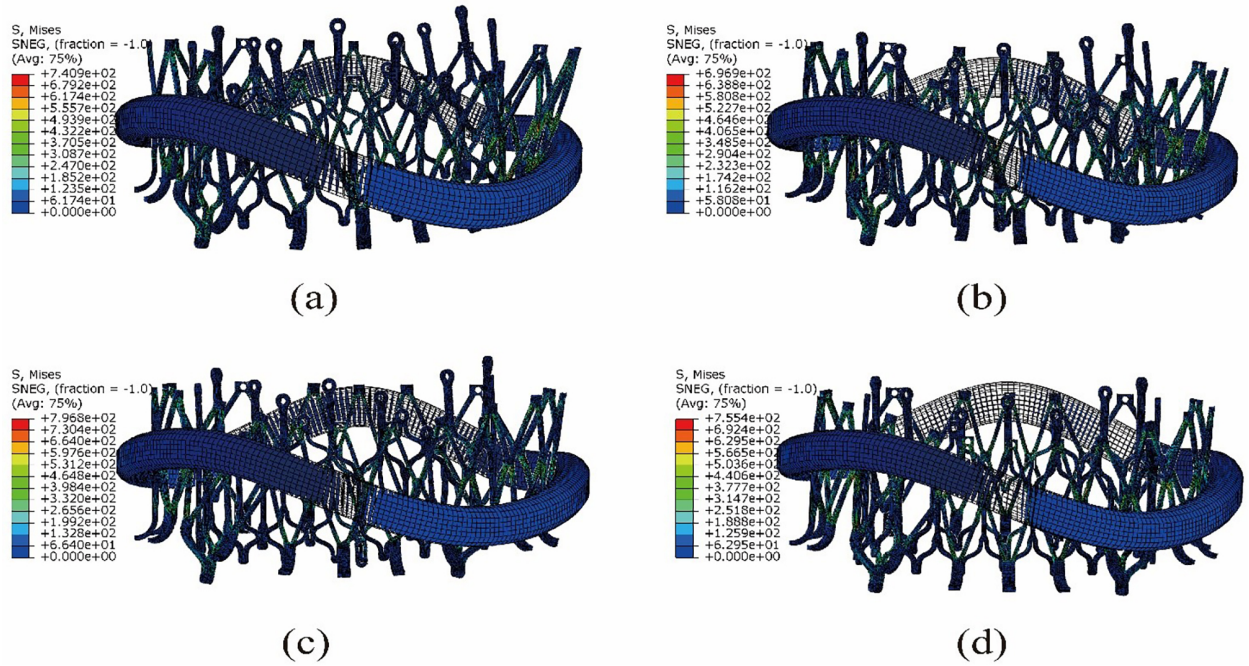

Fig. 8. Stress maps for different annuloplasty ring implantation depths: (a–d) 0, 0.5, 1, and 2 mm, respectively.

spectively, and the maximum displacements of the ventricular fixed strut in the anterior region were 1.3, 1.3, 0.84, and 0.83 mm, respectively.

Stress and Strain Analysis of the Three- and Six-Ventricular Fixed-Strut Stent Structural Connections in the Annuloplasty Ring

The stress forces of the three- and six-ventricular fixed-strut stents implanted at a depth of 0 mm in the annuloplasty ring are shown in Fig. 10. In the three-ventricular fixed-strut stent, when the ventricular fixed-strut lengths was 3, 4, and 5 mm, the maximum stresses in the posterior region were 696, 740, and 830 MPa, respectively, and the maximum stresses in the anterior region were 570, 557, and 621 MPa. In the six-ventricular fixed-strut stent, when the ventricular fixed-strut length was 3, 4, and 5 mm, the maximum stresses in the posterior region were 674, 666, and 644 MPa, and the maximum stresses in the anterior region were 649, 628, and 619 MPa. In addition, the average stresses of the three-ventricular fixed-strut outer stent in the annuloplasty ring were 93, 99, and 104 MPa, respectively, and those of the six-ventricular fixed-strut outer stent were 50, 47, and 90 MPa, respectively.

The cross-sectional morphological strain diagrams of the stent structures with three and six ventricular fixed struts at an implantation depth of 0 mm in the shaping ring are shown in Fig. 11. For the three-ventricular fixed struts, at lengths of 3, 4, and 5 mm, the maximum displacements in the inner layer support strut's posterior ring area were 3.6, 3.7, and 2.9 mm, respectively, while those in the anterior ring area were 2.9, 3.0, and 2.6 mm, respectively. For the six-ventricular fixed-support strut, at lengths of 3, 4, and 5 mm, the maximum displacements in the inner layer support strut's posterior ring area were 3.1, 2.8, and 3.2 mm, respectively, while those in the anterior ring area were 2.3, 2.2, and 2.1 mm, respectively.

Discussion

Three- and Six-Ventricular Fixed Struts Subjected to Blood Pressure and Other Factors

The stress in the posterior junction region is greater than that in the anterior junction region in the three- and six-ventricular fixed-strut stents when subjected to blood pressure and other factors. This may be due to the uneven force on the anterior and posterior ring ventricular fixed struts during compression bending caused by the inconsistent cross-sectional shapes of the inner and outer stents. The stress in the connection region of the six-ventricular fixed-strut stents was approximately half of the corresponding connection region of the three-ventricular fixed-strut stents, which allowed the former to reduce damage during the cardiac cycle.

Because there were three continuous ventricular fixed struts in the anterior region of the six-ventricular fixed-strut stents, the concentrated traction in this region was too large. This causes deformation in which the anterior region of the six-ventricular fixed-strut stents is larger than that of the three-ventricular fixed-strut stents. In the posterior region, owing to the longer distance and the increase in the number of ventricular fixed struts, the deformation of the inner stent of the six-ventricular fixed-strut stent decreased by half compared with the three-ventricular fixed struts.

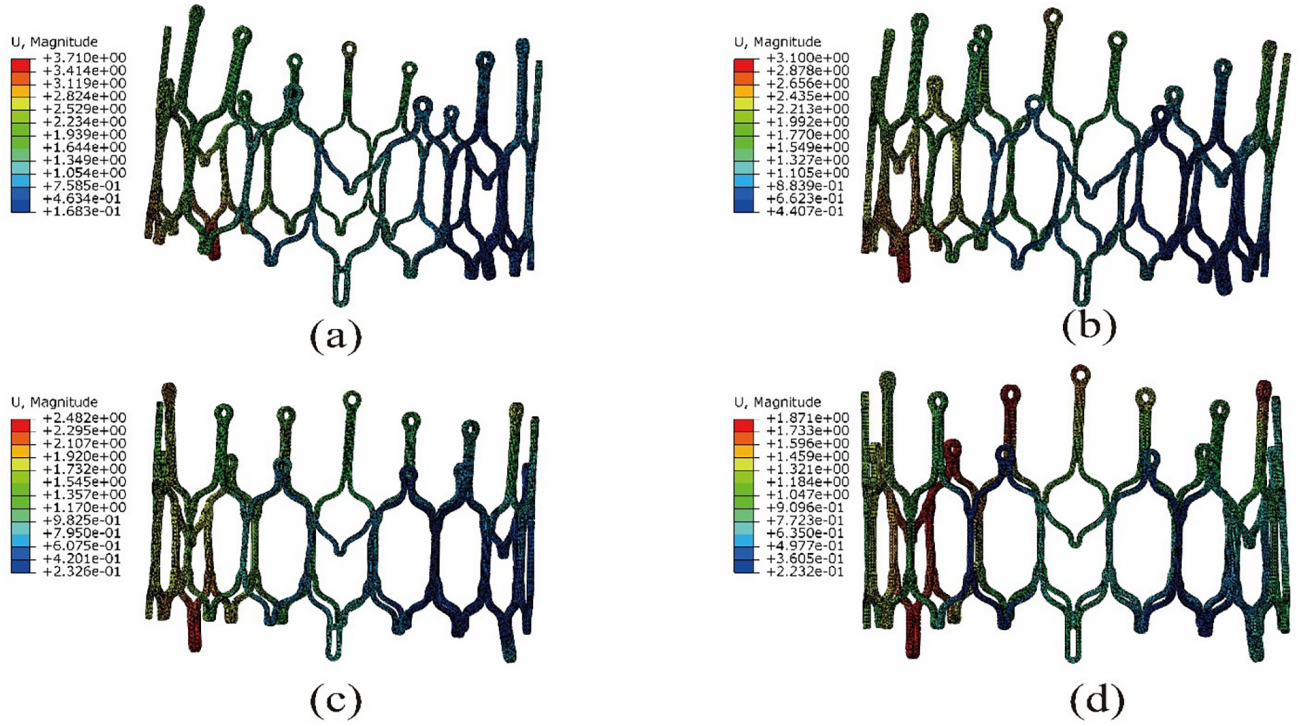

Fig. 9. Strain maps for the inner stent at different annuloplasty ring implantation depths: (a–d) 0, 0.5, 1, and 2 mm, respectively.

In summary, in stent design, it is advisable to appropriately increase the number of ventricular fixation pillars to effectively reduce damage to ventricular support struts. However, the ventricular fixation pole spacing should not be too small, as this can lead to excessive inner stent deformation.

Three-Ventricular Fixed-Strut Stents Implanted at Different Annuloplasty Ring Depths

The maximum stress at an implantation depth of 1 mm was 1.7% higher than that at 0.5 mm. Considering the calculation error, the maximum stress was relatively stable when the implantation depth was <1.5 mm. Although the maximum stress at implantation depths of 0 and 2 mm was approximately 6% higher than that at 0.5 mm, this difference can also be compensated for by an increased fatigue safety factor, considering that the mesh size is less than 0.08. However, because the maximum stress occurs on the right side of the posterior ring, although the implantation depth is believed to cause almost the same stent damage, the right side of the posterior ring of the stent is the most vulnerable to damage and must be considered in the design.

The inner stent displacement was mainly caused by extrusion of the ventricular fixed struts. Therefore, the displacement of the inner stent connected region between the inner stent and ventricular fixed strut was used to represent its strain. The maximum displacement of the right posterior region at insertion depths of 0, 0.5, 1, and 1.5 mm increased by 98.3%, 65.7%, 32.6%, and 14.4%, respectively, compared with that at an insertion depth of 2 mm. Most of the anterior region and left posterior ring displacement was caused by the displacement of the right part of the posterior region, and it was mostly less than 1 mm, which could be overlooked. This is because the right posterior region of the annuloplasty ring is more ventricular-oriented than other regions, resulting in a lower vertical height. Therefore, when the stent is implanted into the ring, the right posterior region ventricular fixation struts act on the ring, resulting in excessive displacement against the inner stent; the rest of the stent is the mesh in contact with the ring. Therefore, the smaller the implantation depth, the greater the impact on the inner stent, which significantly reduces the hemodynamic performance of the stent.

In summary, when implanting a dual-layer stent into the annulus, the implantation depth should be increased to avoid compromising the hemodynamic performance. In the stent design, it is possible to incorporate higher-positioned notches to anchor the stent and improve the anchoring position, thus preventing the ventricular connecting struts from directly contacting the annulus.

Three- and Six-Ventricular Fixed-Strut Structural Connections in the Annuloplasty Ring

The maximum stresses of the three- and six-ventricular fixed struts implanted into the annuloplasty ring were less than the tensile limit for the nitinol alloy (1290 MPa). The maximum stress of the three-ventricular fixed strut with a length of 5 mm was 19% and 12% higher than that of the struts with lengths of 3 and 4 mm, respectively. Therefore, it is believed that when the ventricular fixed struts are small (less than or equal to 3 mm), an increase in

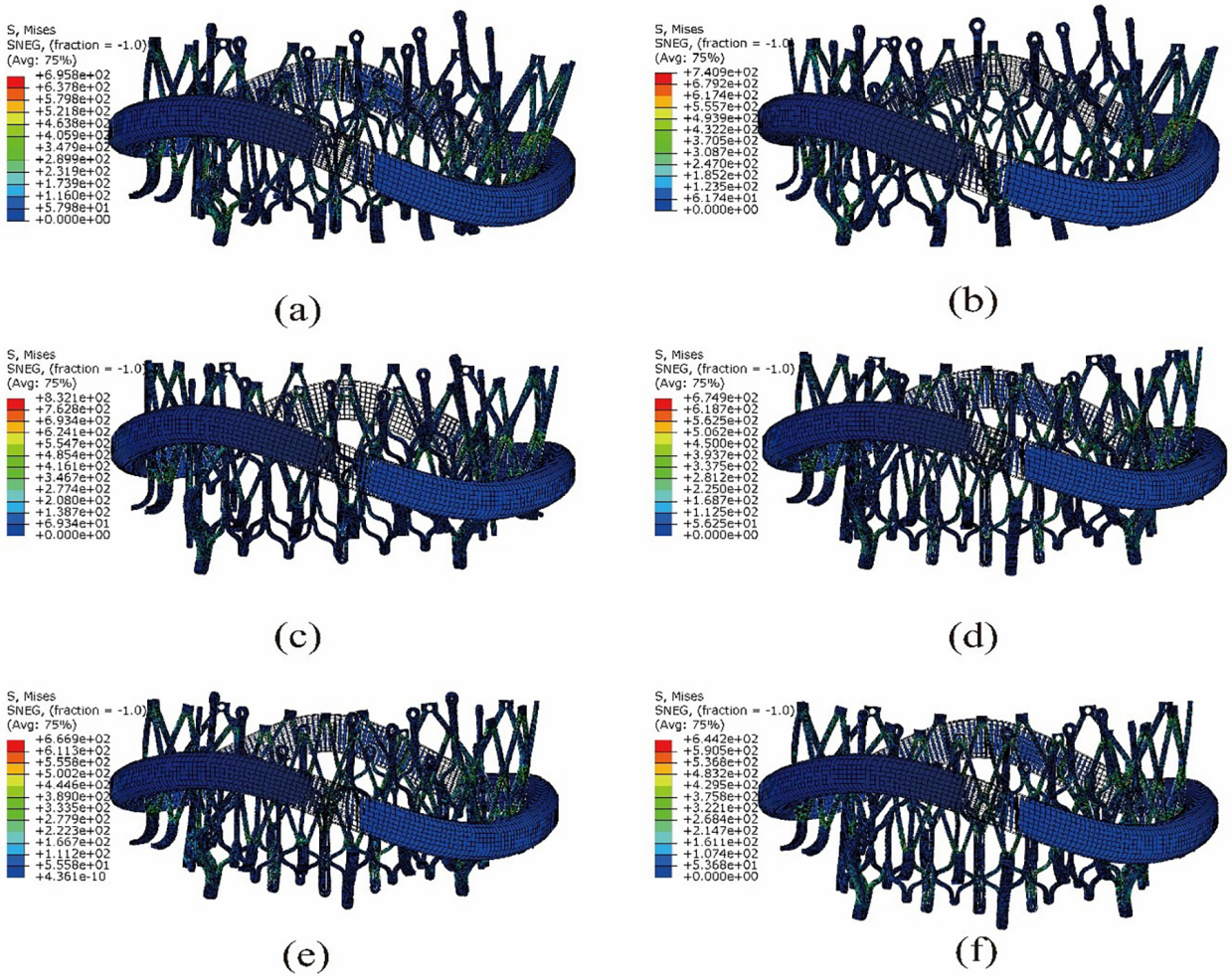

Fig. 10. Stress diagram of double-layer stent implanted into the annuloplasty ring. (a–c) Stress distribution of the three-ventricular fixed-strut stents with lengths of 3, 4, and 5 mm, respectively, implanted at a depth of 0 mm in the annuloplasty ring. (d–f) Stress distribution of the six-ventricular fixed-strut stents with lengths of 3, 4, and 5 mm, respectively, implanted at a depth of 0 mm in the annuloplasty ring.

strut length will increase damage to the posterior region of the stent. The maximum stress of the three-ventricular fixed strut with a length of 5 mm was 4% and 3% less than that of the 3- and 4-mm-long struts, respectively. However, this difference could also be compensated for by an increased fatigue safety factor, considering that the mesh size was less than 0.08. Therefore, when the number of ventricular struts is large, a change in strut length causes relatively stable damage to the stent. Additionally, the maximum pressure in the anterior region of the three- and six-ventricular stents was lower than that in the posterior region, especially in the 5-mm-long three-ventricular stent, and the pressure in the anterior region was 25% lower than that in the posterior region. Therefore, special attention should be paid to the posterior ring area during the design stage.

In summary, owing to the relative stability of the stent compression damage caused by the ventricular fixation strut length within the annulus, it is advisable to appropriately increase this length during the design stage to avoid direct contact with the annulus.

Limitations

When discussing the implantation depth impact on the annuloplasty ring stress and strain, it is assumed that a rigid ring does not undergo deformation. However, in clinical practice, annuloplasty rings are not only rigid but also include flexible and semi-flexible/semi-rigid configurations, which deform under pressure. Additionally, annuloplasty rings undergo deformation during the cardiac cycle due to heartbeats. However, in this study, the effects of these factors on annuloplasty ring deformation and its impact on the stent were not considered. In the next phase of our study, we will consider the native left ventricle and mitral annulus models when investigating flexible and semi-flexible/semi-rigid rings to analyze the results, and we will incorporate flow field simulations to examine the impact of realistic blood flow velocities on the stents.

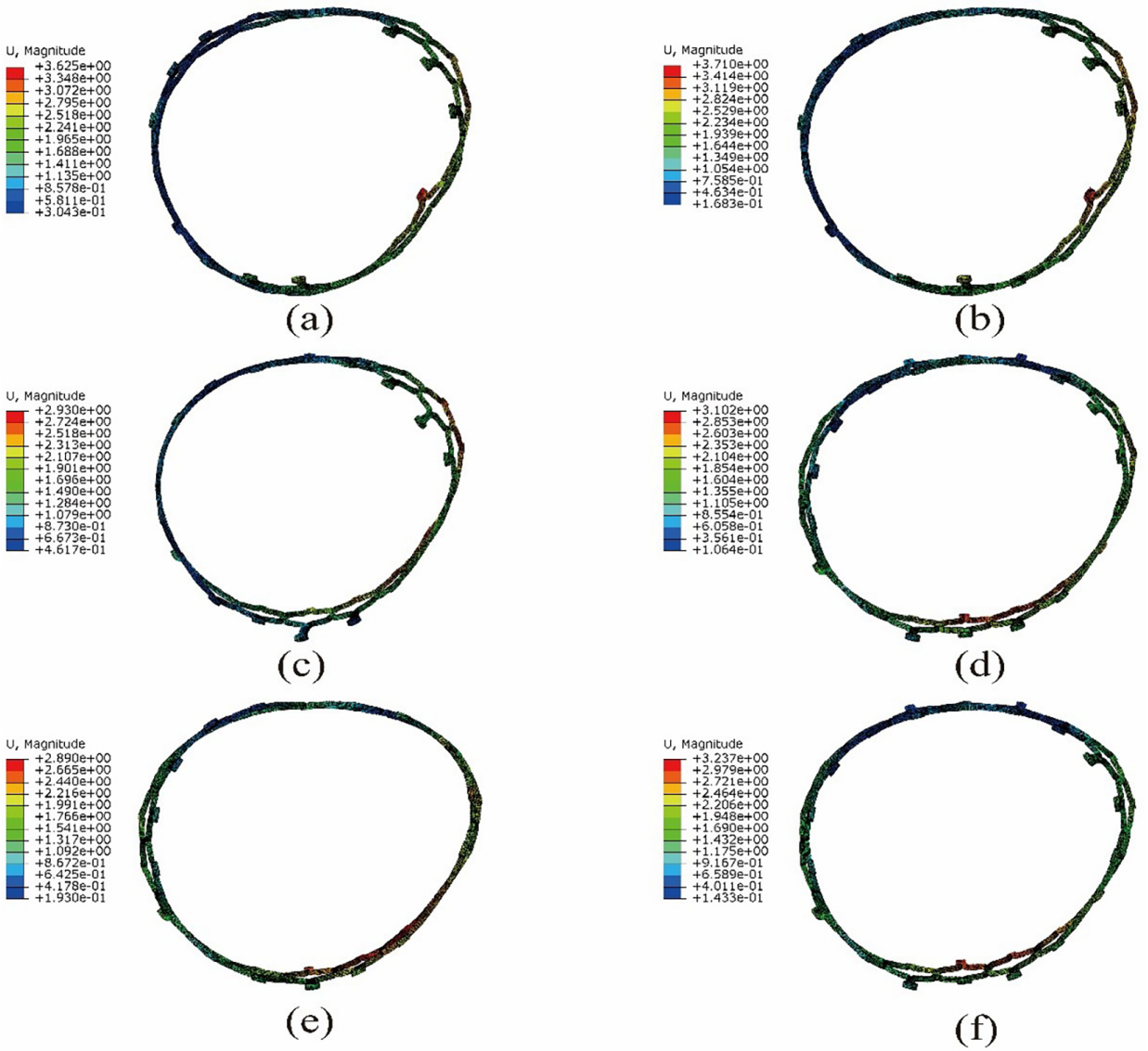

Fig. 11. Displacement diagram of the inner valve stent. (a–c) Cross-sectional morphological strain of the inner stent with three-ventricular fixed struts with lengths of 3, 4, and 5 mm, respectively, at an implantation depth of 0 mm in the annuloplasty ring. (d–f) Cross-sectional morphological strain of the inner stent with six-ventricular fixed struts with lengths of 3, 4, and 5 mm, respectively, at an implantation depth of 0 mm in the annuloplasty ring.

Conclusions

In stent design, it is recommended to appropriately increase the number and length of ventricular fixation columns. when implanting a dual-layer stent into the annulus, the implantation depth should be increased.

Availability of Data and Materials

The data supporting the findings of this study are available from the corresponding author upon reasonable request. The materials used in this study are available upon request from the corresponding author.

Author Contributions

KD: responsible for literature search, scaffold design, simulation experiment design and operation, data analysis, literature review, read and revise the final manuscript. ZH: responsible for proposing solutions to challenging problems, providing guidance, reading and revising the final manuscript, guaranteed the integrity of the experiment and the correctness of the data. Both authors contributed to editorial changes in the manuscript. Both authors have participated sufficiently in the work to take public responsibility for appropriate portions of the content and agreed to be accountable for all aspects of the work in ensuring that questions related to its accuracy or integrity.

Ethics Approval and Consent to Participate

Not applicable.

Acknowledgment

We would like to thank Jian Tan and their assistance in the design of the valve stent.

Funding

This research received no external funding.

Conflict of Interest

The authors declare no conflict of interest.

References

[1] Jedrzejczyk JH, Carlson Hanse L, Javadian S, Skov SN, Hasenkam JM, Thørnild MJ. Mitral Annular Forces and Their Potential Impact on Annuloplasty Ring Selection. Frontiers in Cardiovascular Medicine. 2022; 8: 799994.

[2] Dvir D, Webb J. Mitral valve-in-valve and valve-in-ring: technical aspects and procedural outcomes. EuroIntervention: Journal of EuroPCR in Collaboration with the Working Group on Interventional Cardiology of the European Society of Cardiology. 2016; 12: Y93–Y96.

[3] Bapat V. Valve-in-valve apps: why and how they were developed and how to use them. EuroIntervention: Journal of EuroPCR in Collaboration with the Working Group on Interventional Cardiology of the European Society of Cardiology. 2014; 10: U44–U51.

[4] Sticchi A, Reineke D, Praz F, Windecker S. Transcatheter Mitral Valve Replacement for Mitral Valve-in-Valve, Valve-in-Ring, and Valve-in-MAC Using Balloon-Expandable Transcatheter Heart Valves. JACC. Cardiovascular Interventions. 2021; 14: 873–878.

[5] Eleid MF, Cabalka AK, Williams MR, Whisenant BK, Alli OO, Fam N, *et al*. Percutaneous Transvenous Transseptal Transcatheter Valve Implantation in Failed Bioprosthetic Mitral Valves, Ring Annuloplasty, and Severe Mitral Annular Calcification. JACC. Cardiovascular Interventions. 2016; 9: 1161–1174.

[6] De Backer O, Piazza N, Banai S, Lutter G, Maisano F, Herrmann HC, *et al*. Percutaneous transcatheter mitral valve replacement: an overview of devices in preclinical and early clinical evaluation. Circulation. Cardiovascular Interventions. 2014; 7: 400–409.

[7] Wilson R, McNabney C, Weir-McCall JR, Sellers S, Blanke P, Leipsic JA. Transcatheter Aortic and Mitral Valve Replacements. Radiologic Clinics of North America. 2019; 57: 165–178.

[8] Blanke P, Dvir D, Cheung A, Levine RA, Thompson C, Webb JG, *et al*. Mitral Annular Evaluation With CT in the Context of Transcatheter Mitral Valve Replacement. JACC. Cardiovascular Imaging. 2015; 8: 612–615.

[9] Pierce EL, Bloodworth CH, 4th, Imai A, Okamoto K, Saito Y, Gorman RC, *et al*. Mitral annuloplasty ring flexibility preferentially reduces posterior suture forces. Journal of Biomechanics. 2018; 75: 58–66.

[10] Midha PA, Raghav V, Condado JF, Okafor IU, Lerakis S, Thourani VH, *et al*. Valve Type, Size, and Deployment Location Affect Hemodynamics in an In Vitro Valve-in-Valve Model. JACC. Cardiovascular Interventions. 2016; 9: 1618–1628.

[11] Finotello A, Morganti S, Auricchio F. Finite element analysis of TAVI: Impact of native aortic root computational modeling strategies on simulation outcomes. Medical Engineering & Physics. 2017; 47: 2–12.